Minireview

Molecular mechanism for the crystallization of bacteriorhodopsin in lipidic cubic phases

Peter Nollert[a,b], Hong Qiu[c], Martin Caffrey[c], Jurg P. Rosenbusch[b], Ehud M. Landau[b,d,*]

[a] *Department of Biochemistry and Biophysics, University of California San Francisco, 513 Parnassus, San Francisco, CA 94134-0448, USA*
[b] *Biozentrum, University of Basel, Klingelbergstr. 70, CH-4056 Basel, Switzerland*
[c] *Biochemistry, Biophysics, Chemistry, Ohio State University, 100 W. 18th Avenue, Columbus, OH 43210, USA*
[d] *Department of Physiology and Biophysics, Membrane Protein Laboratory, and Sealy Center for Structural Biology, University of Texas Medical Branch, 301 University Blvd., Galveston, TX 77555-0641, USA*

Received 11 July 2001; accepted 23 July 2001

First published online 6 August 2001

Edited by Andreas Engel and Giorgio Semenza

Abstract Crystals of transmembrane proteins may be grown from detergent solutions or in a matrix of membranous lipid bilayers existing in a liquid crystalline state and forming a cubic phase (in cubo). While crystallization in micellar solutions appears analogous to that for soluble proteins, crystallization in lipidic matrices is poorly understood. As this method was shown to be applicable to several membrane proteins, understanding its mechanism will facilitate a rational design of crystallization, minimizing the laborious screening of a large number of parameters. Using polarization microscopy and low-angle X-ray diffraction, experimental evidence is provided to support a mechanistic model for the in cubo crystallization of bacteriorhodopsin in a lipid matrix. Membrane proteins are thought to reside in curved lipid bilayers, to diffuse into patches of lower curvature and to incorporate into lattices which associate to form highly ordered three-dimensional crystals. Critical testing of this model is necessary to generalize it to other membrane proteins. © 2001 Published by Elsevier Science B.V. on behalf of the Federation of European Biochemical Societies.

Key words: Crystallization; Bacteriorhodopsin; Lipidic cubic phases

1. Introduction

Genomic sequencing has revealed that approximately one third of all genes encode membrane proteins having at least one membrane-spanning helix [1]. A complete understanding of the function of integral membrane proteins requires knowledge of their three-dimensional structure at or near atomic resolution. The major bottleneck en route to obtaining high-resolution structures of membrane proteins is the preparation of diffraction quality single crystals. A paradigm of a membrane protein is the light-driven proton pump, bacteriorhodopsin (bR), with its seven transmembrane helices. bR has long been a target for conventional crystallization using mixed detergent–protein micelles. With one exception [2], this methodology has yielded bR crystals of comparably low diffraction quality, in which the protein is in a functional state markedly different from the native one. In contrast, the recently introduced concept of membrane protein crystallization in lipidic cubic phases [3] has produced crystals of functional bR [4] of exceptional diffraction quality. These have been instrumental in resolving the high-resolution structure of bR in the ground state at increasing resolution [5–8]. These structures reveal the intricate interactions between bR, native purple membrane lipids, and water molecules, in an environment closely resembling that of the cell membrane. Recently, lipidic cubic phase-grown bR crystals were instrumental in yielding high-resolution structures of photocycle intermediates [9–14], which should eventually allow a complete understanding of the proton pumping mechanism of the molecule at the atomic level. Moreover, we have recently demonstrated that bR crystals can also be grown in a lipidic cubic phase directly from the native membrane without exposure to any detergent [15]. Finally, we and others have extended the method and demonstrated that the lipidic matrix used for in cubo (forming a cubic phase) crystallization allows the formation of three-dimensional crystals with membrane proteins differing with respect to the size of their membranous and extramembranous domains [16,17].

Theoretical aspects of lipidic mesophases have been studied in detail [18], but our knowledge of the interactions of membrane proteins with such phases remains limited. Recently, triggered by the success of crystallizing membrane proteins from lipidic cubic phases, a number of reports that discuss issues related to the interaction of membrane proteins with lipidic cubic phases have appeared [19–23].

Using the crystallogenesis of bR, we present experimental evidence in support of a hypothesis for the molecular mechanism of in cubo crystallization, which was originally proposed by Landau and Rosenbusch [3], and later developed further [19–23]. The hypothesis describes how the protein, upon reconstitution into the continuous curved membrane of the cubic phase, traverses its convoluted and highly curved bilayer and eventually forms a lamellar-type packing arrangement within a crystal.

*Corresponding author. Department of Physiology and Biophysics, 301 University Blvd., University of Texas Medical Branch, Galveston, TX 77555-0437, USA. Fax: (1)-409-772 1301.
E-mail address: emlandau@utmb.edu (E.M. Landau).

Abbreviations: bR, bacteriorhodopsin; MO, monoolein; OG, β-octyl glucopyranoside

0014-5793/01/$20.00 © 2001 Published by Elsevier Science B.V. on behalf of the Federation of European Biochemical Societies.
PII: S0014-5793(01)02747-8

2. Material and methods

2.1. bR crystal growth in X-ray capillaries and glass vials

Data reported in Figs. 1, 2, 3 and 5 are from crystallization experiments in glass vials, conducted as described [3]. Data reported in Table 1 and Fig. 4 are from crystallization experiments in capillaries. Monoolein (MO) (monooleoyl-*rac*-glycerol [C18:1c9]) from NuCheck (MN, USA) was mixed with a bR solution (concentrations as in [23]) to form a transparent, highly viscous cubic phase [3,23] using a syringe-based mixer [24], injected into 1 mm quartz capillaries (Supper Inc.) and sealed. This pre-crystallization mix consisted of ca. 60% (w/w) MO and 40% (w/w) bR solution. The final MO concentration of similarly prepared binary MO/water mixtures, determined gravimetrically, was 61.4 ± 1.7% (w/w). bR crystallization in quartz capillaries was initiated by adding 0.3 g finely ground Sørensen salt (94.8 g KH_2PO_4 and 5.2 g $NaH_2PO_4{\cdot}H_2O$) per 1 g of pre-formed cubic phase, or by adding an approximately equal amount of lipidic cubic phase consisting of 60% (w/w) MO and 40% (w/w) water mixed with 0.552 mg Sørensen salt/mg of the pre-crystallization mix.

Crystallization of bR was also induced by partial sample dehydration. For this purpose the pre-crystallization matrix mix, prepared in a glass vial, was incubated with an excess of 0.4 M Sørensen salt solution (pH 5.6) for 2 months. Under these conditions, no bR crystals were observed. The surplus solution was then removed and the lipid matrix was allowed to dry for several minutes, reducing its weight by ca. 4%. Some of the lipid matrix was then filled into capillaries. Crystals grown in glass vials and capillaries were observed by light microscopy.

2.2. Enzymatic digestion and crystal dissolution

Enzymatic digestion of the MO in the lipidic cubic phase was conducted as described [25]. Dissolution was induced by overlaying a crystallization setup containing fully grown crystals with an equal volume of water.

2.3. Low-angle X-ray diffraction

X-rays (1.5418 Å) were generated by a rotating anode (18 kW, RU-300; Rigaku). Sample-to-detector distance (ca. 250 mm) was determined using silver behenate as a standard [26]. Samples were exposed for 30–60 min and diffraction images were collected behind a ca. 1 inch wide slit on a 200×250 mm image plate (Fuji HR-IIIN) and read with a phosphor image scanner (Storm 840) at a resolution of 100 μm/pixel [27]. Powder patterns were integrated radially using FIT2D. Subsequent Gaussian fitting was done using ORIGIN 5.0. The limit of detection of a coexisting second mesophase was estimated to be ca. 5%. All measurements were performed at 21°C in dim red light.

2.4. Calculation of curvature

Based on the assumptions outlined in [28], the average Gaussian curvature K_{ave} was calculated as

$$K_{ave} = 2\pi\chi / A_o a^2 \quad (1)$$

where χ is the Euler–Poincaré characteristic and A_o is the ratio of the minimal surface in a unit cell to the quantity (unit cell volume, a)$^{2/3}$. For a thorough theoretical discussion, see [29]. Values were $A_o = 3.091$, $\chi = -8$ and $A_o = 1.919$, $\chi = -2$ for the cubic-Ia3d and cubic-Pn3m phases, respectively. Lipid length in the cubic-Pn3m phase at 21°C was 17.3 Å [28].

3. Results

3.1. Phenomenology of in cubo crystallization of bR

Prior to crystallization, bR is added to the cubic phase either from a detergent solution [3,23] or in the form of purple membrane [15]. In a typical in cubo crystallization mixture, ~10 purple membrane lipids, ~750 *N*-octyl-β-glucoside, and ~15 000 MO molecules were present per detergent-solubilized bR monomer. The detergent concentration was calculated from the initial concentration in the bR solution, and from the decrease in volume during the concentration step, as described in [3]. The protein is uniformly dispersed throughout the lipid matrix, as evidenced by the homogeneous purple color of the material (Fig. 1A). The protein remains in this state for time periods exceeding years (data not shown). Crystallization is initiated by the addition of solid Sørensen salt. Three-dimensional purple crystals of bR grow within the bulk cubic phase, while the matrix purple color fades visibly. This phase transformation is facilitated by diffusion of bR molecules from the host bulk cubic phase and their incorporation into the growing crystals. The first bR crystals appear in the vicinity of the salt crystals, and as crystallization progresses, crystals form throughout the bulk cubic phase (Fig. 1B). The number of crystals decreases and their size increases as a function of distance from the salt. Crystal growth in cubo is accompanied by the appearance of a small volume of colorless aqueous solution that contains salt crystals in contact with the lipidic cubic phase. Altogether, four distinct macroscopic phases can be observed in the mature samples: (i) colorless lipidic cubic phase, (ii) purple bR crystals, (iii) salt crystals, and (iv) colorless aqueous solution surrounding the salt crystals. Hence, the initially homogeneous two-phase system composed of lipidic cubic phase and salt evolves into a four-phase system.

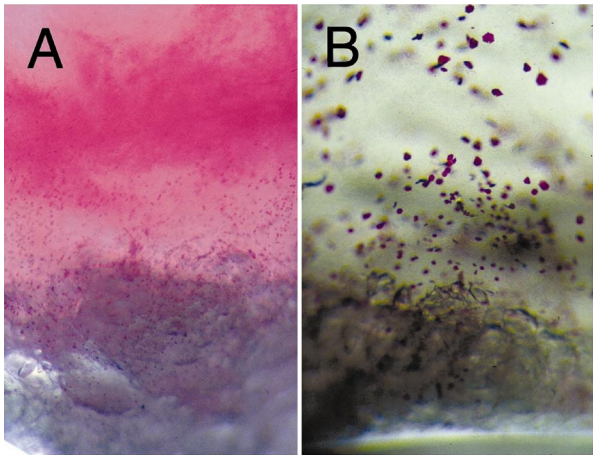

Fig. 1. Microscopic images of the crystallization of bR in the lipidic matrix, conducted as described [3]. The upper and middle parts of each image show the lipidic matrix and bR, lower parts depict solid Sørensen salt. A: Crystallization setup 2 days after addition of the salt. Most of the purple color (bR) is still distributed homogeneously in the lipidic matrix, and some purple microcrystals have started to form close to the Sørensen salt. B: A second crystallization set up after 2 months. bR crystals with sizes up to 40 μm have formed. The crystals are surrounded by a colorless lipidic cubic phase.

Upon microscopic inspection with cross-polarized light, bR crystals appear to have a pink hue and are enveloped by a layer of blue birefringence several micrometers thick, whereas the bulk cubic phase appears non-birefringent (Figs. 2 and 3). The blue birefringence is indicative of a non-isotropic lipidic phase, possibly a lamellar phase [20,21]. It disappears upon enzymatic removal of the host lipid (Fig. 2, inset) [25]. Hence, a physical connection between the protein layers in the crystal and the curved bilayer of the lipidic cubic phase, via a lipid bilayer such as a portal lamellar phase, may exist [20,21].

3.2. Low-angle X-ray diffraction

Bulk phase states of the lipidic matrices containing bR were determined by low-angle X-ray diffraction at different stages

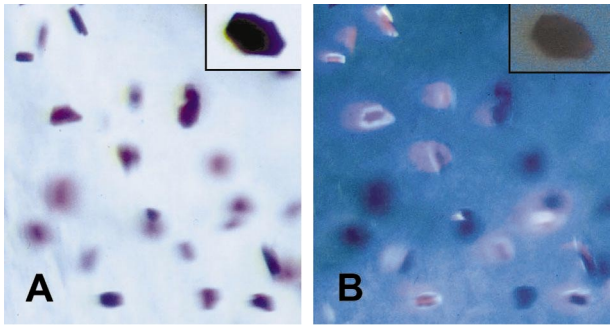

Fig. 2. bR crystals grown in the MO lipidic matrix in glass vials [3] are surrounded by a non-cubic, birefringent lipidic phase. Crystals grown in a MO lipid matrix were viewed using a light microscope without (A) and with (B) crossed polarizers. A: Purple bR crystals are embedded in a colorless, transparent lipid phase. B: Light blue birefringence around bR crystals. A single crystal in water that was removed from the lipidic phase by enzymatic digestion of MO lacks the surrounding blue birefringence (insets on top right section of images A and B). Crystal sizes are ca. 30–40 μm.

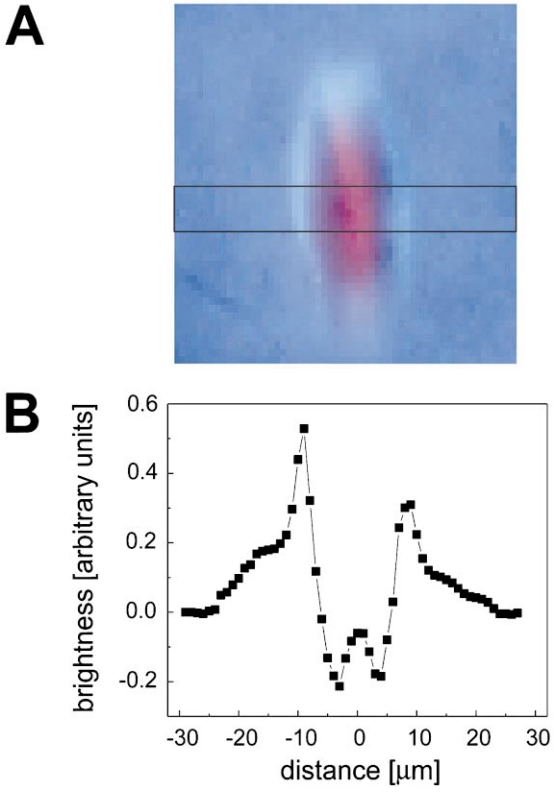

Fig. 3. Analysis of the birefringence surrounding a single bR crystal grown in the lipidic matrix in glass vials [3]. Crystal is viewed edge on, i.e., the large hexagonal *ab* face is perpendicular to the plane of the figure. A: bR crystal surrounded by birefringent glow. The horizontal section used for the quantitative analysis of brightness is marked by a rectangle. The crystal itself exhibits a pink birefringence. The crystal surfaces are darker than the bulk. B: Brightness of section through the crystal. The crystal is ca. 15 μm thick. Two regions that vary in brightness encompass the crystal and protrude ca. 3–5 μm into the lipidic cubic phase on each side. Partial birefringence in lipid phases is commonly caused by crystalline or non-cubic domains.

in the crystallization experiments. Table 1 summarizes the results. Initially, bicontinuous lipidic cubic phases of space groups Pn3m and Ia3d, as well as a lamellar phase, were identified. These phases also occur in binary mixtures of MO and water, for which detailed lyotropic and thermotropic phase diagrams have been established [28,30]. The number, identity of different phases, and their unit cell size at the initial stage of the process depends on the β-octyl glucopyranoside (OG) and Sørensen salt concentrations. High levels of OG favor Lα phase formation. In like manner, the OG homolog, dodecyl maltoside, has been shown to destabilize the cubic mesophase in hydrated MO [31]. Addition of Sørensen salt resulted either in a significant decrease of the cubic phase lattice parameter or in phase transitions prior to appearance of bR crystals. Both phenomena are accompanied by an increase in bilayer curvature. An increase of the initial salt concentration resulted in the pre-crystallization lipid phase being of the cubic-Pn3m type, thereby enabling the entire crystallization process to occur without a lipid phase transition. bR crystals did not form when the crystallization experiment was initiated from a lamellar liquid crystal phase or when the final phase was of the cubic-Ia3d type.

Crystallization experiments were accomplished by adding various amounts of Sørensen salt to the bR-containing MO

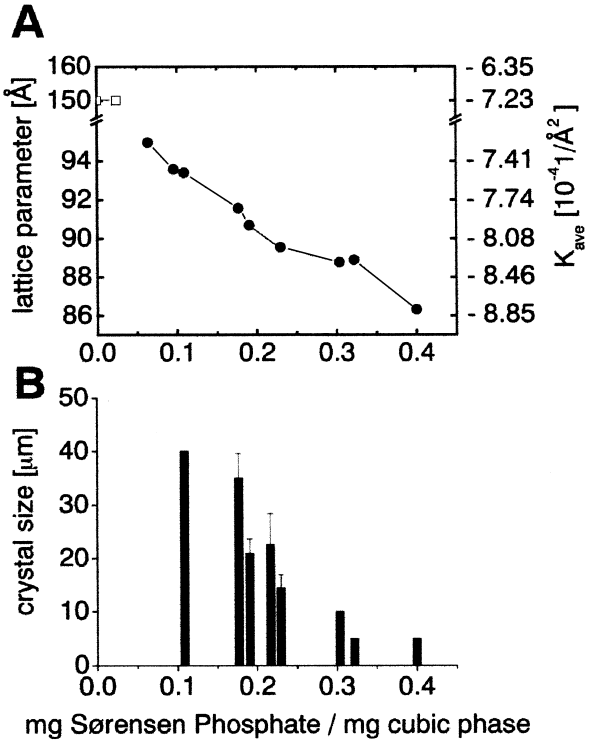

Fig. 4. Effect of Sørensen salt on the phase behavior of MO and on the bR crystal size. These experiments were conducted in capillaries. A: Type and lattice parameter of the lipidic cubic phases, determined by low-angle X-ray diffraction, as a function of Sørensen salt concentration. Filled circles, cubic-Pn3m; open squares, cubic-Ia3d. K_{ave} was calculated using Eq. 1. B: Average bR crystal size as a function of Sørensen salt concentration. Sizes were determined by measuring the longest axis of at least 10 fully grown (>3 months) hexagonal crystals. Error bars show standard deviations. Below an equivalent amount of 0.1 mg salt added to 1 mg pre-crystallization mix, no crystals were observed after 1 year. Note that the Ia3d-to-Pn3m lipid phase transition observed (in A) does not coincide with the onset of bR crystallization (in B).

Table 1
Lipid phases and their lattice parameters, as determined in crystallization experiments

Initial composition of crystallization matrix[a] (crystallization/dissolution treatment)	Result	Mesophase identity and microstructure characteristics					
		initial, before treatment			after treatment		
		phase identity	lattice parameter (Å)	$K_{ave} \times 10^{-4}$ (Å^{-2})	phase identity	lattice parameter (Å)	$K_{ave} \times 10^{-4}$ (Å^{-2})
20 mM Sørensen salt, ca. 0.15 M OG. (addition of solid Sørensen salt[b])	no bR crystals observed	Lα	50	0	Ia3d	140	−8.3
20 mM Sørensen salt, ca. 0.12 M OG. (addition of solid Sørensen salt[b])	bR crystallization	Lα Ia3d	47 140	0 −8.3	Pn3m	87	−8.7
20 mM Sørensen phosphate, ca. 75 mM OG (addition of solid Sørensen salt[b])	bR crystallization	Ia3d	145	−7.7	Pn3m	87	−8.7
300 mM Sørensen salt, ca. 75 mM OG (addition of solid Sørensen salt[b])	bR crystallization	Pn3m	104	−6.1	Pn3m	92	−7.7
Pre-incubation of crystallization matrix[a] with 0.4 M Sørensen salt solution, ca. 75 mM OG (removal of excess solution, partial dehydration)	bR crystallization (Fig. 5)	Pn3m	102	−6.3	Pn3m	87	−8.7
Mature crystallization setup with 3 M Sørensen salt, ca. 75 mM OG (addition of an equal volume of water to a mature crystallization setup containing bR crystals)	bR crystal dissolution	Pn3m	86	−8.9	Pn3m	98	−6.8

Phase identification and microstructure determination were made by low-angle X-ray diffraction. Measurements were performed on samples in quartz capillaries in dim light at 21°C. Representative lattice parameter values are reported.
[a]Pre-crystallization setups contained 60% (w/w) MO, 40% (w/w) protein solution, 3.5 mg bR/ml.
[b]Crystallization was induced by adding the Sørensen salt mixed with MO and water, as described in Section 2.1.

cubic phase (Fig. 4). Below a critical threshold amount of Sørensen salt, no bR crystals formed. The minimum amount of Sørensen salt necessary for crystallization to occur was approximately 0.1 mg salt for 1 mg of pre-crystallization mix. Under these conditions, crystals attained their largest size, and the lattice parameter of the host cubic-Pn3m phase was ca. 93.5 Å, corresponding to an average Gaussian curvature of $-7.5 \cdot 10^{-4}$ Å^{-2}. Dehydration of the lipidic material, starting at either low (100 mM) or high (400 mM) salt concentrations, also yielded micro crystals (Fig. 5), giving rise to a new crystallization procedure, and demonstrating that the ionic strength per se is not solely responsible for bR crystal formation. During dehydration, the loss of water was determined to be only 4% of the total weight. Therefore, the salt concentration increase in the aqueous compartment of the cubic phase is ~8%. Since such crystallization-by-dehydration-experiments can be carried out with a starting concentration varying from 100 to 400 mM, the major crystallization-inducing effect is possibly caused by alterations of the lipidic compartment of the cubic phase, rather than by an increase in the ion concentration of the aqueous compartment.

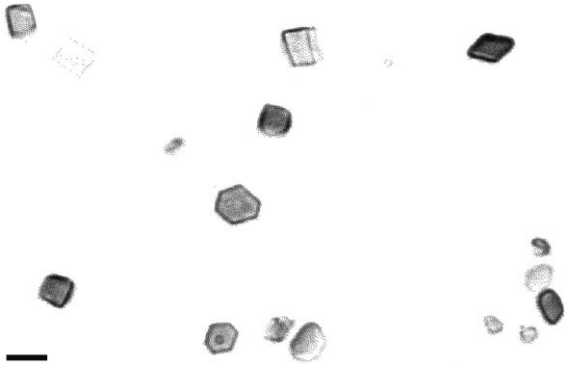

Fig. 5. Collection of bR microcrystals grown by dehydration of the lipidic cubic phase material, in the absence of added Sørensen salt (see Table 1). Hexagonal, cubic and rhomboid crystal morphologies are present along with amorphous shaped objects. Microscopic images were taken with phase contrast optics. Bar represents 5 μm.

4. Discussion

4.1. Crystallization phenomenology in the context of lipidic phase behavior

Our approach to deciphering the mechanism of crystallization of membrane proteins in cubo [3,14–16,19–23] is based on investigating the lyotropic phase behavior of the MO/water system [21,28,30]. Formation of two-dimensional crystalline arrays of bR was shown to require Sørensen salt and was driven by specific interactions between bR and the major anionic purple membrane lipids: 2,3-di-*O*-phytanyl-*sn*-glycero-1-phosphoryl-3′-*sn*-glycerol 1′-phosphate and 2,3-di-*O*-phytanyl-*sn*-glycero-1-phosphoryl-3′-*sn*-glycerol 1′-sulfate [32–34]. Despite the different conditions prevailing in three-dimensional in cubo crystallization, some mechanistic aspects contributing to phase separation into two-dimensional lipid–protein arrays, as predicted by a simple stochastic model [35], and independently by a molecular field theory [36], might apply in cubo. Because all processes required to effect in cubo crystallization as described here are performed at 21°C, the respective isotherm in the temperature–composition phase diagram of the MO/water system can be used as a guideline [21,23,28,30]. At this temperature, the hydrated cubic phase is at or close to full hydration. Upon dehydration,

the bilayer curvature of the cubic phase increases, triggering a cubic-to-lamellar phase transformation at sufficiently low hydration. The membrane protein crystallization experiment can be understood in this context [19–23]: added precipitant competes with the lipid for available water, thereby lowering the activity of water. Thus, the salt effectively destabilizes the cubic phase in favor of a lamellar phase. Crystallization does not require a complete cubic-to-lamellar phase transformation. Rather, the crystallization mechanism calls for a small amount of lamellar phase that may be encountered at the point of phase coexistence. The cubic phase may thus be contiguous with a lamellar phase, acting as an orienting portal for the protein between the feeder cubic phase and the crystal, which acts as a sink.

4.2. Membrane curvature and mismatch

Because the number of MO and water molecules in the in cubo crystallization system far outnumber that of bR molecules, formation of a macroscopically undisturbed cubic phase is possible. On the microscopic level, there are, however, consequences due to the presence of one bR molecule in one out of five unit cells of the Ia3d phase (unit cell dimension, $a = 145$ Å [28]), or in one out of 13 unit cells of the Pn3m ($a = 104$ Å) phase prior to crystallization. The molecular dimensions of bR and the matrix lipid MO are markedly different, both in length (bR, ca. 33 Å; MO, 17.3 Å) and diameter (bR, 25 Å; MO, ~4–5 Å) of the respective hydrophobic, roughly cylindrically shaped moieties (numbers for bR are from RCSB database accession code 1QHJ). Therefore, the precise regular geometric pattern of the bicontinuous cubic phase cannot be maintained in unit cells harboring bR molecules. In the following, we present a qualitative outline of the interactions of membrane proteins with negatively curved membranes such as bicontinuous cubic phases. We conclude that such interactions are least favorable under conditions of high-curvature compared to those between membrane protein and lipids in lamellar-type crystals, thereby constituting the driving force for crystallization in cubo.

The precise location of transmembrane proteins within curved bilayers that constitute the lipidic cubic phase is unknown. However, based on the increased stability of bR in the lipidic matrix and the reasoning outlined in Loewen et al. [20], it is reasonable to assume that the protein is reconstituted into the curved MO bilayer. The protein may be considered to be in a taut state, presumably caused by a curvature-related hydrophobic mismatch at the lipid–protein boundary (schematically shown in Fig. 6). This mismatch is conceptually similar to the one described for wedge-shaped proteins in a bent bilayer [37], which incurs an energy penalty. In contrast, in a planar setting of the correct thickness, such mismatch is minimized (Fig. 6C). Such a penalty is presumably minimized by a local deviation of the membrane curvature from its regular pattern (Fig. 6C). We have demonstrated that an increase in curvature is brought about by the addition of salt to the MO matrix. The described mismatch can be resolved by effecting a phase separation of the host lipidic cubic phase into a highly curved cubic phase lacking membrane defects, and a lamellar crystalline protein array.

4.3. Crystallization model

The mechanism of nucleation and crystal growth of bR in lipidic cubic phases [3,19–23] is proposed to take place in four or five consecutive steps (Fig. 7). Monomeric bR in the micellar state [38] may be treated as a rigid body, and thus possesses six degrees of freedom, three translational and three rotational. Reconstitution into the bilayer of the lipidic cubic phase limits the mobility of the protein; specifically, it reduces the number of degrees of freedom by two rotational and one translational, resulting in a system with a total of three degrees of freedom [39]. The crystallization entropy, which is the entropic penalty of immobilizing particles during crystallization, is therefore partly compensated for by this reconstitution prior to the crystallization process. In the case of crystallization starting with the purple membrane incorporated into the cubic phase [15], reconstitution of two-dimensional purple patches or smaller units, possibly bR monomers, into the three-dimensional membranous network might occur. Cubic phase-incorporated bR molecules are pre-oriented by the bilayer, such that the seven transmembrane α-helices reside

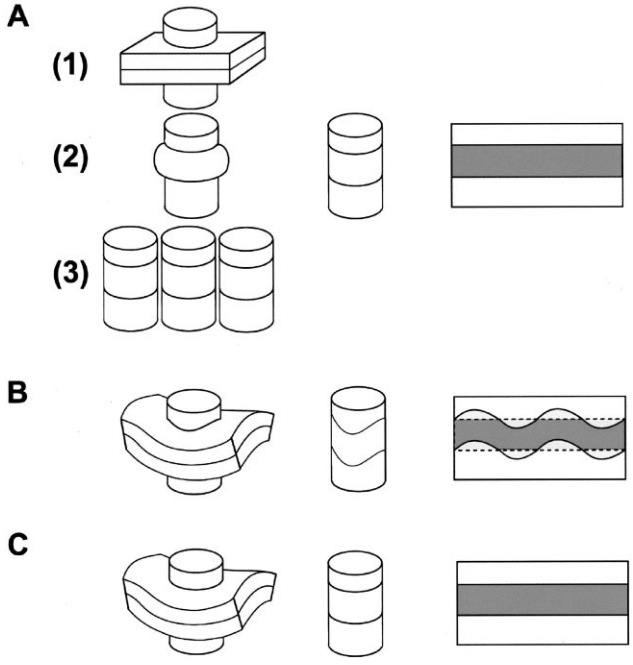

Fig. 6. Hydrophobic matching at the protein–membrane interface in membranous media with diverse curvatures. Membrane proteins are shown schematically as cylinders. Lipid bilayers are depicted as planar or curved structures. To the left they are shown (from the top) in their respective environments. The middle column shows the borders of interaction with the hydrophobic environment. The rectangles in the right column represent rolled-out versions of the cylinder surfaces with their matching hydrophobic surfaces as dark shaded areas. Mismatch between the two surfaces is shown as lightly shaded areas. A: Protein cylinder interacting with (1) a planar membrane; (2) with a detergent girdle around its transmembrane section; and (3) with neighboring protein molecules. These represent bR in a planar lipid bilayer, in a detergent micelle and in the purple membrane crystalline array, respectively. In all three cases, the hydrophobic surface of the transmembrane region of the protein is entirely matched with a complementary hydrophobic surface of lipid, detergent or protein. B: Membrane protein interacting with a negatively curved bilayer such as that of a bicontinuous cubic phase. The transmembrane region of the protein matches partially with the hydrophobic sections of the bilayer. This mismatch is energetically unfavorable and the degree of mismatch may be reduced by a local distortion of the membrane. C: Restored matching of hydrophobic surfaces of the membrane with that of the protein. In order to achieve this, a local membrane distortion is required, causing bending frustration.

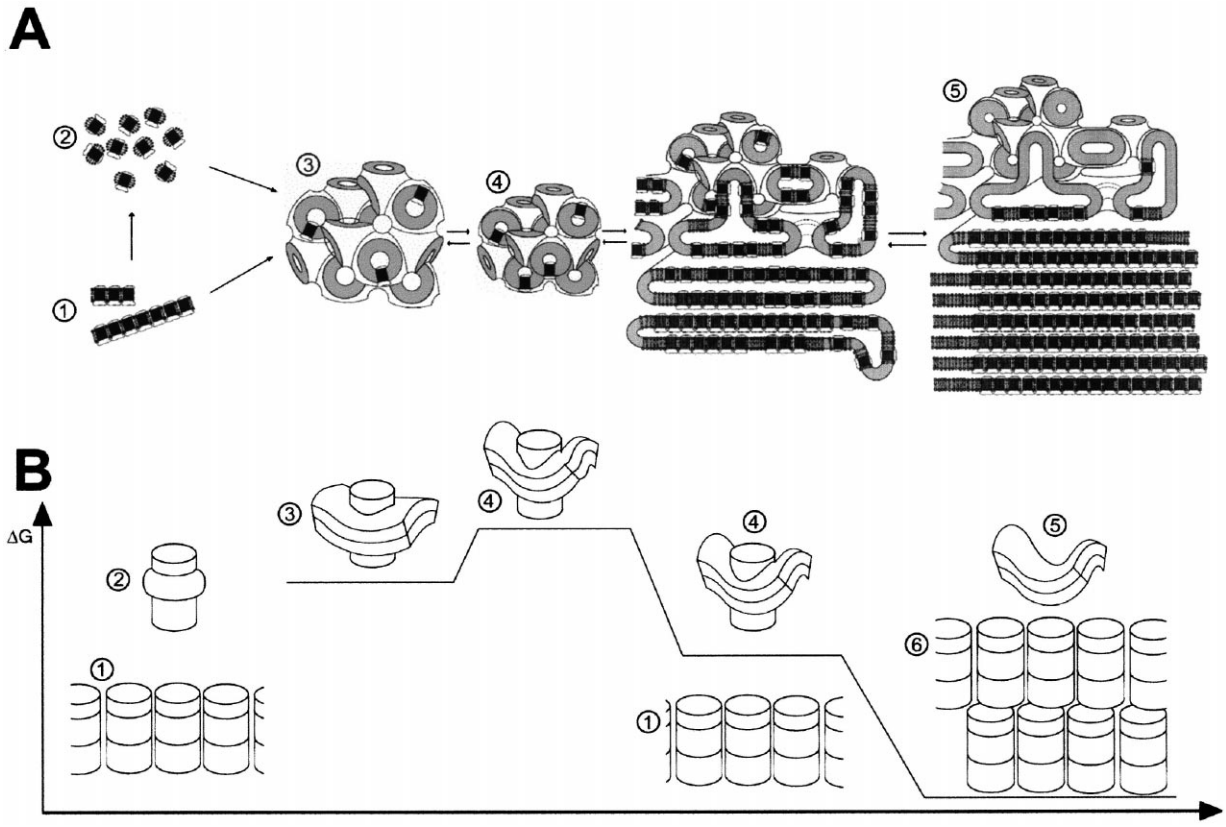

Fig. 7. A hypothesis of the steps leading to the formation of three-dimensional crystals [20,21,23] by incorporation of bR into curved lipid bilayers and subsequent phase separation into lamellar structures. The amphipathic species bR, purple membrane lipids, and detergent partition into the curved membrane of the cubic phase and may diffuse freely therein. Panel A: Schematic description of events occurring during the crystallization of bR in lipidic mesophases. Purple patches (1) or detergent-solubilized monomers (2) insert spontaneously into the curved bilayer (3) of the bicontinuous cubic-Pn3m phase. Addition of Sørensen salt increases the membrane curvature and reduces unit cell size ((3)→(4)). Significant cubic unit cell deformations due to the presence of the protein may occur at this stage. Separation of protein and purple membrane lipid from the highly curved cubic phase bilayer into growing planar domains favors crystal nucleation. Bending frustration is relieved by this process, which occurs by means of lateral diffusion analogously to defect migration and fusion described for similar systems [39]. Diffusion of a misaligned membrane protein along the curved membrane to an adjacent layer may enable a crystallographic match with the growing crystal. Portal lamellae and a putative intermittent sponge phase connect the protein crystal with the surrounding cubic phase. The crystallization process is completed when mature crystals coexist with a bR-depleted and highly curved cubic phase (5). Upon reswelling of the cubic phase by hydration, the crystallization process may be reversed and protein molecules diffuse back into the curved bilayer via the portal lamellae. Panel B: Schematic representation of the various states of protein–membrane interactions encountered during the crystallization process (see also Fig. 6), and the changes in free energy (ΔG).

within the hydrophobic core of the membrane, and the loop regions are solubilized in the aqueous channels. Moreover, the lateral diffusion pathways are defined by the structure of the curved lipid bilayer. This greatly increases the ratio of productive to non-productive protein encounters that are necessary for crystal nucleation and growth.

As outlined in Fig. 6, the presence of planar patches of membrane protein molecules in the bilayer of the cubic phase is incompatible with the geometric constraints of the curved membrane. Accordingly, we postulate the formation of local curvature defects surrounding the embedded membrane protein. Similar local curvature distortions in comparable systems were shown to diffuse and to merge with each other, thereby decreasing the curvature distortion [40]. Furthermore, curvature-induced particle concentration in a bilayer has been described on a theoretical basis for a similar system [41]. Analogously, we reason that a curvature-induced aggregation of bR and purple membrane lipids occurs above a certain threshold. Partitioning of bR molecules into an adjacent local planar domain relieves strain. In cases where the protein is tightly bound to native lipids, it may be escorted by native lipids through the entire crystallization process. bR exhibits this type of lipidic chaperoning [42] and we suggest that the tendency of purple membrane lipids to form planar sheets [43] contributes to nucleation of this phase separation. Crystal growth in the lipid–protein plane may be envisaged by lateral merging of protein and of small purple membrane-like units, guided by the matrix bilayer. Indeed, a recent statistical thermodynamics analysis of membrane bending-mediated protein–protein interaction revealed that, in the regime of negative Gaussian curvature, the interactions between proteins are attractive [44]. The structure of the portal membrane may resemble that of phase transition intermediates, as observed in bicontinuous cubic-to-lamellar phase transitions [45], in membrane fusion [46], or in sponge phases [47]. Interestingly, coexistence of the cubic-Pn3m phase with lamellar structures of the Lα type has not been identified in the pure, two-component MO/water model system [30]. The high-resolution structure of bR reveals hexagonal packing of trimers in the *a–b* plane, while adjacent planes are related by a two-fold

screw axis along the c-direction, forming polar $P6_3$ crystals [5]. Crystallographic and mass spectroscopic analyses of the crystals have revealed the presence of at least four different lipid species and their precise location within and around the bR trimer [7,8]. Thus, protein molecules and purple membrane lipids are arranged in lamellar sheets in the crystal, adopting the same orientation with respect to the membrane plane as that assumed by bR in the native membrane. Negative charges on the hydrophilic surface of the AB and the BC loops and of purple membrane lipid must be screened by cations in order to establish the crystal contacts along the *c*-axis. The weak contacts along this axis are manifested by the tendency of bR crystals to form twinned crystals [6]. This type of twinning may be overcome by appropriate crystallization conditions [7].

This model explains the macroscopic, as well as the microscopic, phenomena associated with bR crystallization in the lipidic matrix. Consistent with the presence of a lamellar membranous network connecting crystal and bicontinuous cubic phase is the observation that dissolution of bR crystals can be induced by slightly rehydrating the cubic phase (Table 1).

4.4. Concluding remarks

The proposed mechanism is based on experiments with bR as outlined above, and its extension to and validity for other proteins should be tested. For example, replacing the curvature-increasing agent (Sørensen salt) in crystallization experiments by others, such as polyethylene glycol [48] should lead to crystal formation. Indeed, bR crystals can be grown in a cubic matrix by slow dehydration (Fig. 5). Conversely, an increase in pressure that decreases membrane curvature [49] should facilitate crystal dissolution. For the proteins that have so far been crystallized in cubo [3,16,17], we expect to identify different curvature thresholds due to their disparate size and transmembrane shape. Finally, we expect that additional examples of membrane protein crystals grown in cubo will reveal packing arrangements similar to that of bR. According to the model proposed here, layered packing is uniquely compatible with a physical feeding portal connecting the crystalline protein moieties with the surrounding bicontinuous lipidic cubic phase.

The content of and packing arrangement in bR crystals demonstrates that care needs to be taken during purification of membrane proteins in order to prevent total delipidation. Alternatively, addition of affine lipids to crystallization systems may prove beneficial. We envisage that these insights will form a basis for successful crystallization of membrane proteins in cubo, en route to determining their structures in association with lipids.

The mechanism described here, and in the literature [3,19–23], provides a qualitative explanation of the process of crystal nucleation and growth. A thorough quantitative understanding of the energetics of interaction of curved membranes with embedded membrane proteins must be established in order to describe precisely the intricate details of the crystallization process. Nonetheless, membrane protein crystallization trials along the lines of the in cubo strategy may profit from the insight gained already on this descriptive level.

5. Note added in proof

Recently, the in cubo crystallization approach yielded well-diffracting crystals of sensory rhodopsin II, the structure of which was solved independently by two groups to 2.1 Å resolution [50] and 2.4 Å resolution [51].

Acknowledgements: We thank G. Büldt for purple membrane and A. Hardmeyer for excellent technical assistance. Discussions with V. Cherezov, M. Chiu, M. Engelhard, A. Gulik, V. Luzzati, J. Navarro, D. Siegel and R. Templer are greatly appreciated. Supported in part by Grants from the Human Frontiers Research Science Organization to P.N. (LT0156/1999-M); the National Institutes of Health (GM 56969, GM 61060) and the National Science Foundation (DIR 9016683, DBI 9981990) to M.C.; the Swiss National Science Foundation's SPP BIOTECH (5002-46092, 5002-55179) to J.P.R. and E.M.L; and the EU-BIOTECH (PL 970415) to E.M.L. The support of the Howard Hughes Medical Institute to the Membrane Protein Laboratory at UTMB is greatly appreciated.

References

[1] Wallin, E. and von Heijne, G. (1998) Protein Sci. 7, 1029–1038.
[2] Essen, L.-O., Siegert, R., Lehmannn, W. and Oesterhelt, D. (1998) Proc. Natl. Acad. Sci. USA 95, 11673–11678.
[3] Landau, E.M. and Rosenbusch, J.P. (1996) Proc. Natl. Acad. Sci. USA 93, 14532–14535.
[4] Heberle, J., Büldt, G., Koglin, E., Rosenbusch, J.P. and Landau, E.M. (1998) J. Mol. Biol. 281, 587–592.
[5] Pebay-Peyroula, E., Rummel, G., Rosenbusch, J.P. and Landau, E.M. (1997) Science 277, 1676–1681.
[6] Luecke, H., Richter, H.T. and Lanyi, J.K. (1998) Science 280, 1934–1937.
[7] Belrhali, H., Nollert, P., Royant, A., Menzel, C., Rosenbusch, J.P., Landau, E.M. and Pebay-Peyroula, E. (1999) Structure 7, 909–917.
[8] Luecke, H., Schobert, B., Richter, H.T., Cartailler, J.P. and Lanyi, J.K. (1999) J. Mol. Biol. 291, 899–911.
[9] Edman, K., Nollert, P., Royant, A., Belrhali, H., Pebay-Peyroula, E., Hajdu, J., Neutze, R. and Landau, E.M. (1999) Nature 401, 822–826.
[10] Luecke, H., Schobert, B., Richter, H.T., Cartailler, J.P. and Lanyi, J.K. (1999) Science 286, 255–260.
[11] Royant, A., Edman, K., Ursby, T., Pebay-Peyroula, E., Landau, E.M. and Neutze, R. (2000) Nature 406, 645–648.
[12] Luecke, H., Schobert, B., Cartailler, J.P., Richter, H.T., Rosengarth, A., Needleman, R. and Lanyi, J.K. (2000) J. Mol. Biol. 300, 1237–1255.
[13] Sass, H.J., Büldt, G., Gessenich, R., Hehn, D., Neff, D., Schlesinger, R., Berendzen, J. and Ormos, P. (2000) Nature 406, 649–653.
[14] Pebay-Peyroula, E., Neutze, R. and Landau, E.M. (2000) Biochim. Biophys. Acta 1460, 119–132.
[15] Nollert, P., Belhali, H., Pebay-Peyroula, E. and Landau, E.M. (1999) FEBS Lett. 457, 205–208.
[16] Chiu, M.L., Nollert, P., Loewen, M.C., Belrhali, H., Pebay-Peyroula, E., Rosenbusch, J.P. and Landau, E.M. (2000) Acta Cryst. D 56, 781–784.
[17] Kolbe, B., Besir, H., Essen, L.-O. and Oesterhelt, D. (2000) Science 288, 1390–1396.
[18] Templer, R.H. (1998) Cur. Opin. Coll. Interf. Sci. 3, 255–263.
[19] Landau, E.M. (1998) in: Biomembrane Structures (P.I. Haris and D. Chapman, Eds.), pp. 23–38, IOS Press, Amsterdam.
[20] Loewen, M., Chiu, M.L., Widmer, C., Landau, E.M., Rosenbusch, J.P. and Nollert, P. (1999) in: G protein-coupled receptors. CRC Methods in Signal Transduction Series (Haga, T. and Berstein, G., Eds.), pp. 365–388, CRC Press, Boca Raton, FL.
[21] Caffrey, M. (2000) Curr. Opin. Struct. Biol. 10, 486–497.
[22] Nollert, P., Navarro, J. and Landau, E.M. (2001) in: G Protein Pathways, Methods in Enzymology (Iyengar, R. and Hildebrandt, J.D., Eds.), in press, Academic Press, San Diego, CA.
[23] Rummel, G., Hardmeyer, A., Widmer, C., Chiu, M.L., Nollert, P., Locher, K.P., Pedruzzi, I., Landau, E.M. and Rosenbusch, J.P. (1998) J. Struct. Biol. 121, 82–91.
[24] Cheng, A., Hummel, B., Qiu, H. and Caffrey, M. (1998) Chem. Phys. Lipids 95, 11–21.

[25] Nollert, P. and Landau, E.M. (1998) Biochem. Soc. Trans. 26, 709–713.
[26] Blanton, T.N., Huang, T.C., Toraya, H., Hubbard, C.R., Robie, S.B., Louër, D., Göbel, H.E., Will, G., Gilles, R. and Raftery, T. (1995) Powder Diffr. 10, 91–95.
[27] Zhu, T. and Caffrey, M. (1993) Biophys. J. 65, 939–954.
[28] Briggs, J., Chung, H. and Caffrey, M. (1996) J. Phys. II 6, 723–751.
[29] Templer, R.H., Seddon, J.M., Duesing, P.M., Winter, R. and Erbes, J. (1998) J. Phys. Chem. B 102, 7262–7271.
[30] Qiu, H. and Caffrey, M. (2000) Biomaterials 21, 223–234.
[31] Ai, X. and Caffrey, M. (2000) Biophys. J. 79, 394–405.
[32] Watts, A., Sternberg, B., Ulrich, A.S., Whiteway, C.A., Seifert, G., Sami, M., Fisher, P., Heyn, M.P. and Wallat, I. (1995) Biophys. Chem. 56, 41–46.
[33] Watts, A. (1995) Biophys. Chem. 55, 137–151.
[34] Sternberg, B., Lhostis, C., Whiteway, C.A. and Watts, A. (1992) Biochim. Biophys. Acta 1108, 21–30.
[35] Sabra, M.C., Uitedaag, J.C.M. and Watts, A. (1998) Biophys. J. 75, 1180–1188.
[36] Marèelia, S. (1976) Biochim. Biophys. Acta 455, 1–7.
[37] Kim, K.S., Neu, J. and Oster, G. (1998) Biophys. J. 75, 2274–2291.
[38] Lustig, A., Engel, A., Tsiotis, G., Landau, E.M. and Baschong, W. (2000) Biochim. Biophys. Acta 1464, 199–206.
[39] Ben-Tal, N., Ben-Shaul, A., Nicholls, A. and Honig, B. (1996) Biophys. J. 70, 1803–1812.
[40] Charitat, T. and Fourcade, B. (1997) J. Phys. II 7, 15–35.
[41] Odell, E. and Oster, G. (1994) Lect. Math. Life Sci. 24, 23–36.
[42] Dumas, F., Sperotto, M.M., Lebrun, M.C., Tocanne, J.F. and Mouritsen, O.G. (1997) Biophys. J. 73, 1940–1953.
[43] Jackson, M.B. and Sturtevant, J.M. (1978) Biochem. 17, 4470–4473.
[44] Chou, T., Kim, K.S., and Oster, G. (2001) Biophys. J., in the press.
[45] Clerc, M., Levelut, A.M. and Sadoc, J.F. (1991) J. Phys. II France 1, 1263–1276.
[46] Siegel, D.P. (1986) Chem. Phys. Lipids 42, 279–301.
[47] Hyde, S.T. (1997) Langmuir 13, 842–851.
[48] Chung, H. and Caffrey, M. (1994) Nature 368, 224–226.
[49] Mariani, P., Paci, B., Bosecke, P., Ferrero, C., Lornezen, M. and Caciuffo, R. (1996) Phys. Rev. E 54, 5840–5843.
[50] Royant, A., Nollert, P., Edman, K., Neutze, R., Landau, E.M., Pebay-Peyroula, E. and Navarro, J. (2001) Proc. Natl. Acad. Sci. USA, in press.
[51] Luecke, H., Schobert, B., Lanyi, J.K., Spudich, E.N. and Spudich, J.L. (2001) Science, in press.